JOURNAL OF SOLID STATE CHEMISTRY 88, 217–228 (1990)

Calculation of Orbital Moments in Solids

BARBARA SZPUNAR AND VEDENE H. SMITH, JR.

Department of Chemistry, Queen's University, Kingston, Ontario K7L 3N6, Canada

Received May 23, 1990

DEDICATED TO J. M. HONIG ON THE OCCASION OF HIS 65TH BIRTHDAY

Two methods for the calculation of orbital moments are discussed. In particular previous calculations for YCo_5 with the recursion method are compared to a new linear muffin–tin orbital atomic sphere approximation (LMTO–ASA) calculation. The magnetic properties of YCo_5 are discussed with emphasis on contributions of the different cobalt atom sites (3*g* and 2*c*). The effect of magnetocrystalline anisotropy is discussed. The orbital moment contribution is calculated for $CaCuO_2$,the parent of the new superconducting cuprates. © 1990 Academic Press, Inc.

1. Introduction

In the present study we will concentrate on the properties of transition metal atoms in solids. The electronic structure of transition metal atoms consists of practically inactive core electrons, $4s^2$ electrons, and an incomplete shell of 3*d* electrons. In a solid a transition metal loses its two *s* electrons and becomes a positive ion. Since the 3*d* electrons form an incomplete shell they might lead to a substantial orbital moment contribution to the magnetic moment. For example, since the basic level of Co^{2+} (which has seven *d* electrons) is $^4F_{9/2}$ (*1*) one should expect an orbital moment of the order of 3.0 μ_B (*1*). However, the experimental value of the orbital moment of pure bulk cobalt (*2*) (with hcp crystal structure) is only 0.1472 μ_B. This effect is known as quenching of the orbital angular momentum of transition metals. In a nonuniform, crystal field the angular momentum component in a certain direction (e.g., m_z) is no longer constant and even might average to zero.

It is even more interesting to study the orbital moment of cobalt in compounds. YCo_5 is quite peculiar, since the magnetocrystalline anisotropy of this compound is 10 times higher than that of pure cobalt, even though pure yttrium is in a spin singlet state and isotropic. This compound is of interest because it is representative of intermetallic rare earth transition metal compounds, known to be useful as permanent magnets (*2*). The discovery of $SmCo_5$ (*2*), a compound with extremely large magnetocrystalline anisotropy, opened a new area in the search for permanent magnets. Due to the relatively high cost of the constituents, mass production of $SmCo_5$ never occurred. More recently it has been found that by including boron atoms, one can obtain stable compounds of iron and rare earth metals with large magnetocrystalline anisotropies. In particular, $Nd_2Fe_{14}B$ seems to be the permanent magnet material of the future (*3*).

The crystal structure of $Nd_2Fe_{14}B$ is very complicated and first principles (ab initio) calculations are very time consuming be-

0022-4596/90 $3.00

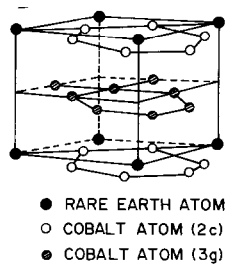

FIG 1. RCo_5 unit cell ($CaCu_5$ crystal structure).

cause there are 68 atoms per unit cell (*4*). However, these compounds have a tetragonal crystallographic structure which is related to the hexagonal $CaCu_5$ structure (*5*) shown in Fig. 1. As a result it is hoped that realistic progress in understanding the magnetic properties of these very complex compounds may be made by an accurate analysis of R(rare-earth)Co_5 compounds.

The first calculations of the magnetic properties of such a compound, YCo_5, were made (*6*) using the self-consistent augmented plane-wave (APW) method (*7*). In those calculations the assumption of equivalence of both types of cobalt sites (Co(2*c*) and Co(3*g*)) (see Fig. 1) meant that the results could not predict a local magnetic anisotropy. It is known from a polarized neutron diffraction study (*8*) that there is a significant difference between these two sites (as revealed in the local spin and orbital moments). In addition, NMR measurements suggest that a competitive anisotropy may exist between these two types of cobalt sites (*9*). Theoretical calculations (*10*) by means of the recursion method (*11*) of the local orbital moments on the two cobalt sites support the experimental results. On the other hand Kurihare *et al.* (*12*) have calculated anisotropy constants for YCo_5 by considering only *d* bands with spin–orbit (s–o) interaction included and find that there is very poor agreement with the experimental data unless it is assumed that there are very small differences ($\approx 10^{-3}$) in the number of electrons for different magnetization directions.

It is the purpose of the present study to investigate this problem by means of electronic structure calculations wherein these cobalt sites are not constrained to be equivalent. The methods employed are discussed in the next two sections while the results are presented and discussed in the following sections.

We also present calculations of the orbital moment in $CaCuO_2$, a compound which is related to high temperature superconductors.

2. The Recursion Method

As discussed above the most important electrons in transition metal atoms are the *d* electrons. Since they are much more localized than the *p* or *s* electrons the Hamiltonian may be simplified such that only hopping terms to nearest neighbors need to be taken into account. This model is called the tight binding method. In addition Heine *et al.* (*13*) proposed the use of an orthonormal basis set in which the Hamiltonian becomes a tridiagonal matrix. This led to a savings in the computer memory required and the Green's function ($G(\varepsilon)$) is of the form of the continued fraction:

$$G_{00}(\varepsilon) = \cfrac{b_0^2}{\varepsilon - a_0 - \cfrac{b_1^2}{\cdots t(\varepsilon)}}, \qquad (1)$$

where a_i, b_i are calculated coefficients and $t(\varepsilon)$ is a terminator which when chosen properly might improve the calculations even further. In our calculations (*10*) we used real angular momentum wave functions, clusters with about 5000 atoms, and 16 levels of the continued fraction expansion. To allow for the magnetic ordering we simply used the Hubbard model in the Hartree–Fock approximation (*14*) which leads to the shift of energy for spin up and spin down electrons respectively by

TABLE I

REAL REPRESENTATION OF THE ANGULAR MOMENTUM WAVE FUNCTIONS FOR d AND p ELECTRONS

$\|m\|$	$\Psi_{2\|m\|}$	$\|m\|$	$\Psi_{1\|m\|}$
2	$\sqrt{15/4}\,(x^2 - y^2)/r^2$, $\sqrt{15}\,xy/r^2$	1	$\sqrt{3}\,x/r$, $\sqrt{3}\,y/r$
1	$\sqrt{15}\,xz/r^2$, $\sqrt{15}\,yz/r^2$	0	$\sqrt{3}\,z/r$
0	$\sqrt{5}\,(z^2 - 1/2(x^2 + y^2))/r^2$		

$$\Delta_s = U\langle n_{-s}\rangle, \tag{2}$$

where U is the effective intraatomic Coulomb energy and $\langle n_{-s}\rangle$ is the average number of electrons with opposite spin. At low temperatures the spin–flip interaction can be neglected and the above equation is used separately for spin up and spin down electrons until a self-consistent solution is obtained for the magnetic moment:

$$m_s = \tfrac{1}{2} g_s \mu_B (\langle n_s\rangle - \langle n_{-s}\rangle). \tag{3}$$

So far in this treatment spin–orbit interaction is not taken into account and the states are doubly degenerate with respect to the sign of the azimuthal quantum number. This leads to a reduction of the number of orbitals used in the calculations and real spherical harmonics are a convenient choice. In Table I the real angular momentum wave functions for $l = 2$ (d electrons) and for $l = 1$ (p electrons) are shown. The choice of spherical harmonics is particularly convenient for orbital moment calculations as has been demonstrated previously (*15*).

The spin–orbit splitting for transition metals is usually small and thus it is sufficient to take it into account non-self-consistently in the last iteration (*16*). A convenient method of introducing this effect in tight binding methods has been proposed previously (*15*). The spin–orbit interaction is

$$\Delta(\mathrm{so}) = \xi \mathbf{l}.\mathbf{s} \tag{4}$$

where $\mathbf{l}$ and $\mathbf{s}$ are the orbital and spin moment operators respectively and ξ is the spin–orbit coupling constant. It becomes very simple in the real spherical harmonic representation (*17*):

$$\Delta(\mathrm{so})^{(j=l+1/2)} = l(\xi/2) \tag{5}$$
$$\Delta(\mathrm{so})^{(j=l-1/2)} = -(l+1)(\xi/2).$$

Using Clebsch–Gordon coefficients (*18*) we can decompose our wave functions as follows:

for $j = l + \frac{1}{2}$

$$m_j = m + \tfrac{1}{2},\ -(l+1) \le m \le l$$
$$\Psi_{jm_jl} = 1/(2l+1)^{1/2}\,(\sqrt{l+m+1}\,\Psi^{\uparrow}_{lm} + \sqrt{l-m}\,\Psi^{\downarrow}_{lm+1}), \tag{6}$$

and for $j = l - \frac{1}{2}$

$$m_j = m + \tfrac{1}{2},\ -l \le m \le l-1$$
$$\Psi_{jm_jl} = 1/(2l+1)^{1/2}\,(\sqrt{l-m}\,\Psi^{\uparrow}_{lm} - \sqrt{l+m+1}\,\Psi^{\downarrow}_{lm+1}.) \tag{7}$$

Our wave functions are degenerate with respect to the sign of m. A simple approximate method of obtaining the density of states with spin–orbit interaction included is to shift the decomposed density of states by the corresponding Δ(s–o) energy (*15*) for corresponding j, m_j, l. In Table II we present explicitly the corresponding decomposition coefficients for the density of states of d and p electrons. The orbital moment can then be calculated from the formula:

$$m_l = g\mu_B \sum_{m=-2}^{2} m \int_{-\infty}^{\epsilon_F} \rho_l^m(\omega)\, d\omega. \tag{8}$$

It is easy to notice from Table II that summation of the weighted splittings within one orbital $l|m|s$ is zero, thus in general we should not expect a change of the position of the Fermi energy after splitting. However, in the case of strongly varying density of states around the Fermi energy the self-consistently adjusted Fermi energy should be found. Also from Table II we can check that in the case of small spin polarization, the spin–orbit splitting contribution for any

TABLE II

PROPORTION OF d AND p ELECTRONS RESPECTIVELY FOR SPIN UP AND DOWN AND DIFFERENT m VALUES ($j = l \pm 1/2$)

	Spin up		Spin down			Spin up		Spin down	
m	$j = 2.5$	$j = 1.5$	$j = 2.5$	$j = 1.5$	m	$j = 1.5$	$j = 0.5$	$j = 1.5$	$j = 0.5$
−2	1/10	4/10	1/2	0	−1	1/3	2/3	1	0
2	1/2	0	1/10	4/10	1	1	0	1/3	2/3
−1	2/10	3/10	4/10	1/10	0	2/3	1/3	2/3	1/3
1	4/10	1/10	2/10	3/10					
0	3/5	2/5	3/5	2/5					

lm orbital is close to the value for both spin up and spin down density of states of electrons but with opposite sign. The only possibility to obtain a substantial orbital moment contribution in this case is through the presence of some nonuniform feature of the density of states around the Fermi energy. This implies that a very high accuracy in the density of states and the position of Fermi energy is required in this case.

3. The LMTO–ASA Method

The LMTO–ASA method, based on local density-functional theory, is known to be a quite good approximation for closely packed systems and has been successfully used for rare earth and transition metals (*19–21*). It has been shown recently (*21*) that it leads to a simple first-principles tight-binding method. The advantage of the LMTO–ASA method is that the transfer matrix factorizes with canonical structure constants which are energy independent and need to be calculated only once for a given crystal structure and set of potential parameters describing the atomic spheres. This feature of the method makes self-consistent calculations less time-consuming and allows one to perform calculations for fairly complicated crystal structures.

In the present calculations we employ a valence basis set of s, p, d, (f) electrons with the frozen core approximation. Argon-like cores have been used for the cobalt, calcium, and copper atoms, krypton-like ones for the yttrium atoms, and helium-like ones for the oxygen atoms. The von Barth–Hedin local (spin) density approximation was used to describe the exchange-correlation energy (*22*). In the self-consistency iterations the spin–orbit coupling was neglected but all other quasi-relativistic effects were included. After self-consistency in the charge and spin distribution has been reached, spin–orbit coupling was included in the final iteration (*23*). The pseudo-perturbational method has been used (*19*) by just adding the spin–orbit term as a perturbation into the Hamiltonian with the spherical potential; $v(r)$ (notation as in Ref. (*19*)):

$$\xi(\mathbf{s}.\mathbf{l}) = c^{-2} 2/r\, dv(\mathrm{r})/dr\, \tfrac{1}{2} \begin{pmatrix} \mathrm{l}_z & \mathrm{l}_- \\ \mathrm{l}_+ & -\mathrm{l}_z \end{pmatrix}. \quad (9)$$

This approximation has been used successfully in our previous paper (*23*) for orbital moment calculations for pure cobalt.

4a. Local Orbital Moments in YCo_5

First we discuss a self-consistent quasi-relativistic calculation of the electronic structure in YCo_5 in which spin-orbit coupling was not included. Our calculations are similar to those of Malik *et al.* (*6*) for YCo_5

except that we have allowed the previously mentioned distinction between the different cobalt sites.

Convergence is very difficult to obtain for YCo_5. This has been noticed previously (*6*), and it is even more difficult when one permits the two types of cobalt sites to be different. Convergence was obtained only by assuming a small mixing parameter (5%) in the iterative process. Ninety points were sampled in the irreducible wedge of the Brillouin zone and the density of states (DOS) was integrated with an energy step of 0.5 mRy.

f electrons were included as part of the valence shell on the cobalt sites. In order to investigate their influence, an additional iteration after convergence was performed without including the *f* electrons. The results for the local magnetic moments were not very dependent on inclusion of higher *l* expansion contributions.

In Figs. 2–4 the local DOS are presented for the Co(2*c*), Co(3*g*), and *Y* sites, respectively. In Fig. 5 the total DOS per atom is shown. The previously mentioned problem in obtaining convergence is probably due to the high DOS of the minority spin electrons at the Fermi energy. In fact the peak of the minority spin density of states is at the Fermi energy. This result is in agreement with experimental expectations (*24*) and also with previous calculations (*6, 14*).

It is known that in some RCo_5 compounds metamagnetism for the cobalt atoms is observed and the external magnetic field can change drastically the local moment on cobalt (*25*). It appears that cobalt, in forming a compound with rare earth metals, changes from a strong to a weak ferromagnet. As can be seen from Table III, the cobalt spin moment in YCo_5, 1.29 μ_B for Co(2*c*) and 1.44 μ_B for Co(3*g*), is reduced in comparison with the moment per cobalt atom for the ideal hcp structure of pure cobalt calculated with the same method. The calculated moment for cobalt atoms in the hcp structure

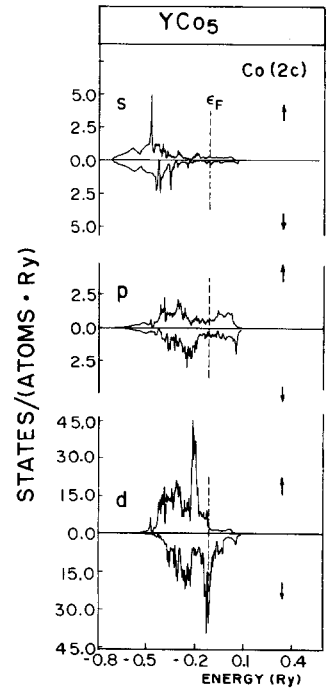

FIG. 2. Local density of states per atom for Co(2*c*) sites in YCo_5 for spin up and down electrons, respectively: *s* electrons, *p* electrons, *d* electrons.

of pure cobalt varied between 1.5 and 1.49 μ_B (*23*) with changes of the *c*/*a* ratio and between 1.55 and 1.49 μ_B with variation of the lattice parameters (*26*). These trends help to explain the reduction of the cobalt moment in YCo_5 in comparison with that in pure hcp cobalt.

It is commonly believed (*27*) that the reduction of the cobalt moment in rare earth–cobalt compounds is due to charge transfer from the rare earth metal to cobalt. The present results do not support this idea since they show the opposite charge transfer. It must be pointed out, however, that charge transfer in a compound is not a well-defined quantity and, in both our calculations and those of Malik *et al.* (*6*), it is dependent on the assumed values of the atomic sphere radii. In our ASA calculations overlapping spheres were used while Malik *et al.*

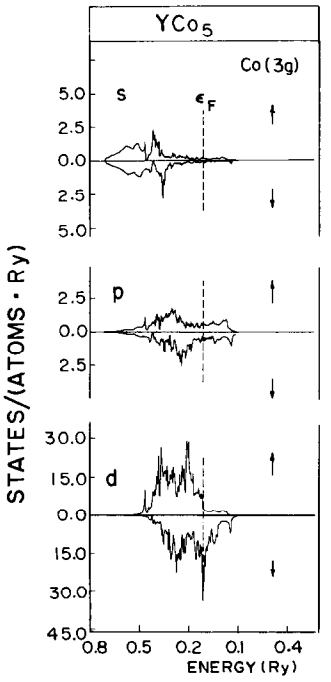

FIG. 3. Local density of states per atom for Co(3g) sites in YCo_5 for spin up and down electrons, respectively: s electrons, p electrons, d electrons.

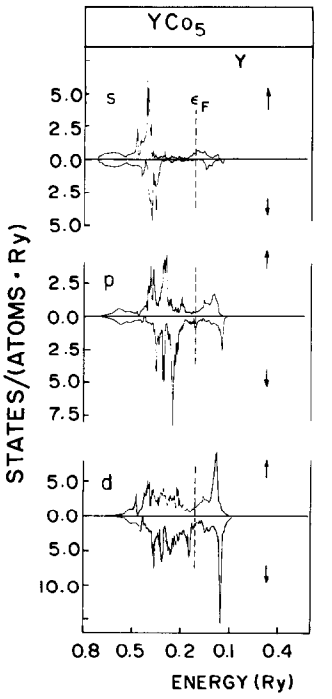

FIG. 4. Local density of states per atom for yttrium sites in YCo_5 for spin up and down electrons, respectively: s electrons, p electrons, d electrons.

(*6*) used nonoverlapping, touching spheres. We have chosen the radii of the atomic spheres to be the atomic sphere radius in pure cobalt and pure yttrium, respectively. They were adjusted so that the equilibrium pressure value should be close to zero. A slightly larger sphere radius was assumed on Co(2c) because a higher orbital moment is expected on this site and it is known that spin–orbit interaction expands the lattice parameters (*28*). The atomic sphere radii utilized were R[Co(2c)] = 2.56 a.u., R[Co(3g)] = 2.52 a.u., and R[Y] = 3.60 a.u. We believe that the charge transfer model can be misleading because there are also other important factors such as the local crystal symmetry, the lattice constants, or the c/a ratio which can affect the magnetic moment values.

Experimental values for the spin and or-

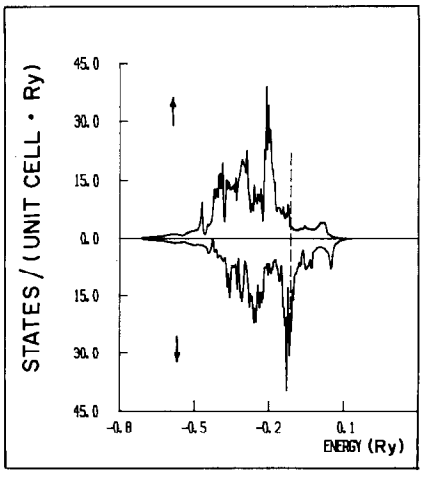

FIG. 5. Total density of states per atom for YCo_5 for spin up and down electrons.

TABLE III

LOCAL SPIN MAGNET MOMENTS (μ_B), CHARGE DENSITIES (e), AND $n(\varepsilon_F)$

Site	s	p	d	f	Total
		Magnet moment/atom			
Co(2c)	−0.0005	−0.0399	1.3315	0.0004	1.2915
Co(3g)	−0.0032	−0.0279	1.4719	0.0038	1.4445
Y	−0.0298	−0.0786	−0.2651	—	−0.3734
		Charge atom			
Co(2c)↑	0.3203	0.3258	4.4131	0.0326	5.0918
Co(2c)↓	0.3208	0.3657	3.0816	0.0322	3.8003
Co(3g)↑	0.3250	0.3135	4.4677	0.0319	5.1381
Co(3g)↓	0.3282	0.3414	2.9958	0.0281	3.6936
Y↑	0.3203	0.4752	0.8781	—	1.6737
Y↓	0.3501	0.5538	1.1432	—	2.0471
		$n(\varepsilon_F)$			
Co(2c)↑	0.2204	0.5085	2.5546	0.0334	3.3169
Co(2c)↓	0.1630	0.4304	38.3706	0.1533	39.1173
Co(3g)↑	0.1319	0.5130	2.8126	0.0197	3.4772
Co(3g)↓	0.0387	0.4520	12.8100	0.1751	13.4758
Y↑	0.3992	0.2952	1.1118	—	1.8062
Y↓	0.0751	0.6064	1.9978	—	2.6793

bital contributions to the local moment (*8*) for the 2c and 3g sites are the following: $m_s^{2c} = 1.31\ \mu_B$, $m_o^{2c} = 0.46 \pm 0.09\ \mu_B$, $m_s^{3g} = 1.445\ \mu_B$, and $m_o^{3g} = 0.275 \pm 0.07\ \mu_B$. The present spin contributions to the magnetic moment are in very good agreement with these experimental values as can be seen from Table III. We obtained a non-zero spin moment on the yttrium site in agreement with previous calculations by Malik *et al.* (*6*). They found the 4d electron contributions to the magnetic moment on the yttrium site to be equal to 0.3 μ_B. A non-zero moment on the yttrium site was obtained in the recursion method calculations (*14*). Due to the higher hybridization of spin down electrons of yttrium with the minority spin d electrons of cobalt, a negative polarization on yttrium was found. This is induced magnetization and all s, p, and d electrons have negative magnetic moments on yttrium in agreement with what has been shown analytically (*14*).

In Figs. 6 and 7 energy band structures are presented for spin up and spin down electrons for different symmetry directions. There is not much difference between the band structure of pure cobalt (*26*) and that of YCo_5. The number of occupied d states is almost the same (pure cobalt $n_{d\uparrow\downarrow} = 7.515$ (*26*) but in YCo_5 the minority d bands of cobalt are squeezed to lower energies due to changes of lattice parameters and hybridization with the yttrium d electrons. The main difference between the two different cobalt sites is that the DOS at the Fermi energy on Co(2c) is higher than on Co(3g) (cf. Figs. 2 and 3, bottom panels). In Fig. 8 we present the local DOS for d electrons on cobalt sites calculated without distinction between the two types of cobalt sites. We can see that similarly to Co(3g) in this case the minority peak at the Fermi level is lower than the corresponding peak on the 2c site. This is probably responsible for the differences in the orbital moment and local anisotropy contribution. Thus in anisotropy calculations we should distinguish between 2c and 3g sites as well as consider aspherical effects in the charge density.

As mentioned above, the polarized neutron diffraction study (*8*) revealed a large difference between the local orbital moments of cobalt on the 2c and 3g sites ($m_o^{2c} = 0.46 \pm 0.09\ \mu_B$, $m_o^3 = 0.275 \pm 0.07\ \mu_B$). Using the method described in Section 2 in our earlier calculations (*10*) we obtained $m_o^{2c} = 0.17$ and $0.25\ \mu_B$ and $m_o^{3g} = 0.04$ and $0.09\ \mu_B$ for two different choices for the spin–orbit interaction coupling constants of 0.0034 and 0.005 Ry, respectively. These values are smaller than the neutron diffraction measurements but NMR measurements by Streever (*9*) of the anisotropy of the orbital moment, $\Delta m(L) = m_{o\parallel} - m_{o\perp}$, give smaller values namely $0.092\ \mu_B$ for the 2c site and $-0.042\ \mu_B$ for the 3g site.

We note that both the tight binding model and the LMTO–ASA method do not take into account fully the effect of asphericity of the electron charge density. In order to

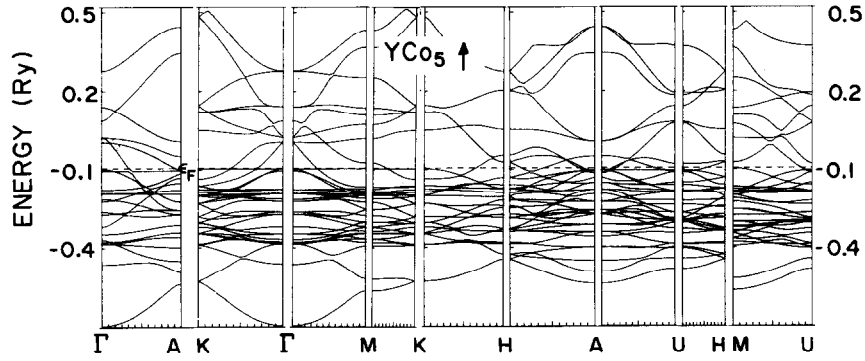

6. Energy band structure of YCo_5 for spin up electrons.

eliminate some of the accumulated error due to the spherical approximation, we should calculate the difference between the local orbital moments on these two sites. In addition we note that the orbital moment values on the cobalt sites are very sensitive to the assumed Fermi energy which was adjusted self-consistently. The Fermi energy shifts from the value -0.1134 Ry without inclusion of spin–orbit coupling to a higher value of -0.0963 Ry with spin–orbit coupling included.

In Fig. 9 we present fully quasi-relativistic calculations of the energy band structure in YCo_5. Since spin–orbit interaction couples spin up and spin down states, we have to diagonalize the full Hamiltonian matrix. Both the spin up and spin down bands are shown on Fig. 9. To calculate the orbital moment we make a projection of the states into *lm* space. The projected density of states for $m_z = \pm 2$ on the Co($3g$) and Co($2c$) sites is presented in Fig. 10, left and right panels, respectively. There are two remarkable peaks on the Co($2C$) site for $m_z = 2$. These peaks are the main contribution to the orbital moment on the Co($2c$) site. The peak closer to the Fermi energy is due to the minority electron peak on this site.

We obtained the difference between local orbital moment on the $2c$ and $3g$ sites to be

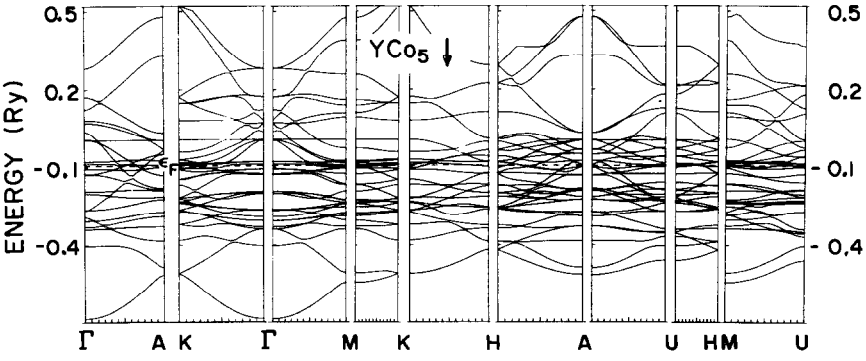

7. Energy band structure of YCo_5 for spin down electrons.

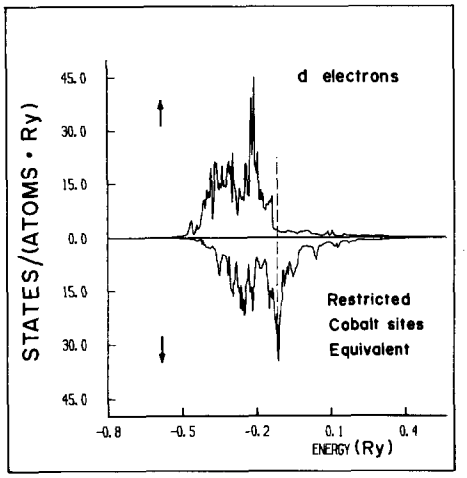

FIG. 8. Local d electron density of states per atom for the cobalt sites in YCo_5 calculated with forced equivalency of the two types of cobalt sites (Co($2c$), Co($3g$)).

equal to $\Delta m_o = 0.18\ \mu_B$. The main contribution to this difference of the orbital moment comes from the d electrons with azimuthal orbital quantum number m_z equal to ± 2. The d electron contribution on site $2c$ is in agreement with our previous calculations (*10*) and equals $0.17\ \mu_B$ but on the $3g$ site we found at present small negative d electron contribution ($-0.04\ \mu_B$) while in semiempirical calculations we find a small positive orbital moment; 0.04 and 0.09 μ_B. In both cases we had to adjust the Fermi energy value due to strong features in the density of states at the Fermi energy for the cobalt atoms.

4b. Orbital Moment Calculations for $CaCuO_2$, the Parent of the Cuprate Family of High T_c Superconductors

It is known by now that LSD approximation has difficulties in obtaining magnetic ordering in the insulating phases related to high T_c superconductors (*29*). Since these difficulties arose one speculation was that possibly the orbital moment might stabilize magnetic ordering in these compounds (*30*). The recently discovered compound (*31*), $CaCuO_2$, is the $n \to \infty$ limit of the series $Bi_2Sr_2Ca_{n-1}Cu_nO_{4+n}$. It is ideal for orbital moment calculations since it has a smaller unit cell (only one CuO_2 layer per unit cell) and thus is tractable with spin–orbit interaction included. In Fig. 11 we show the unit cell of $CaCuO_2$ ($a = 3.86$ and $c = 3.2$ Å) (*31*) together with the important orbitals around the Fermi energy: $d_x2_{-y}2$ on copper sites and one orbital per oxygen site p_x or p_y depending in which direction is the closest copper atom. We performed first LMTO–ASA calculations with all quasi-relativistic effects included except s–o interaction until self-consistency in the charge distribution has been obtained. The atomic sphere radii were chosen as R[Cu] = 2.3 a.u., R[O] = 2.57 a.u., R[Ca] = 3.13 a.u.

It is impossible to create stable magnetic ordering in this compound within the local spin density functional approximation. Even a metamagnetic solution is very unstable, so that we had to keep a large external field in order to create small spin polarization on copper atoms. Then as above we included s–o pseudo-pertubationally in the last iteration and calculated the orbital moment. We find no contribution to the formation of the orbital moment within the accuracy of our calculation.

An intuitive explanation may be based on the fact that in the new high T_c superconductors all states around the Fermi energy are "in plane" states with maximum azimuthal quantum number corresponding to the l_z quantum number (*32*) and the corresponding orbitals are shown schematically on Fig. 11. Since the orbital moment operator is antisymmetric with respect to the sign change of the x or y components for copper atoms there is zero orbital moment contribution from $d_x2_{-y}2$ orbitals (on a square lattice). It might be argued that in La_2CuO_4, due to the interaction of the CuO_2 planes with apical

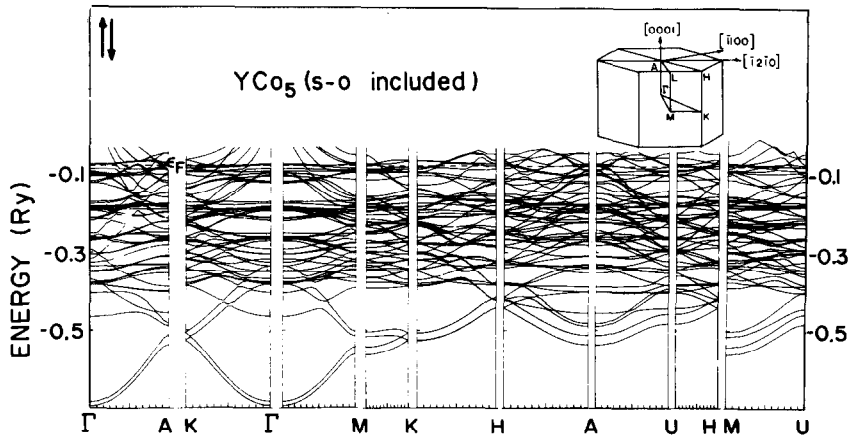

FIG. 9. The quasi-relativistic energy band structure in YCo_5.

oxygens, there would be non-zero orbital moments on Cu. After our work was completed we learned (*33*) that in this case as well zero orbital moment contributions have been found.

4. Implications of the Orbital Moment Calculations for the Magnetocrystalline Anisotropy

The first magnetocrystalline anisotropy calculation from first principles was due to Brooks (*34*). By introducing spin–orbit interaction one would find a small variation in the dependence of the energy on the direction of the magnetic moment. This is the one-ion contribution to the magnetocrystalline anisotropy which usually is the dominant part. In this study we shall concentrate also on the one-ion anisotropy contribution. To estimate the anisotropy Brooks (*34*) calculated the difference in energy for two perpendicular directions of magnetism using perturbation theory. He found satisfactory agreement with experiments for nickel and iron.

To calculate anisotropy from first principles one should perform fully relativistic band structure calculations for different directions of the applied magnetic field. In hexagonal types of structure the magnetic space group is different for magnetization parallel to the [0001] and [1010] directions (*35*). As a result one needs to consider different Brillouin zones for different directions of magnetization.

One must be aware also of the fact that the anisotropic energy contribution is very small and below the accuracy of our calculations. As has been pointed out recently thousands of k points have to be used in order to obtain convergence for anisotropy constants (*36*). Kurihare *et al.* (*12*) do not seem to have realized how small the contribution of the anisotropy energy is to the total energy. In their calculation of the YCo_5 anisotropy they obtained the wrong sign for the value of the anisotropy constant unless "feeble" differences in the electron occupation were introduced for different directions of magnetization. However, they assumed very small differences in the number of electrons but it is apparent from simple calculations that even these contribute to the anisotropy energy significantly. From their results (*12*) we find at the Fermi energy ($\varepsilon_F \approx 0.2$ Ry), the density of states; $N(\varepsilon_F) \approx 100$ electrons/Ry/unit cell and that the "feeble"

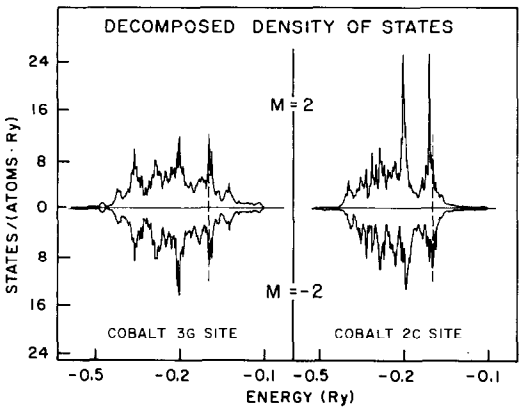

FIG. 10. The decomposed local density of states for $m = 2$ and $m = -2$ on the Co($3g$) and Co($2c$) sites as indicated.

change of electron number $\Delta n \approx 1.0*10^{-3}e$ corresponds to $\Delta E \approx 2*10^{-4}$ Ry/unit cell. An energy difference of 2.10^{-4} Ry/unit cell leads to a difference ΔK in K, the anisotropy constant of $5.2*10^{-7}$ erg/cm^3. Thus the anisotropy they obtained is strictly artificial. On the other hand these calculations give us a good picture about the accuracy required in anisotropy calculations.

The other work which explores the model Hamiltonian proposed by Callaway (*16*) for $3d$ transition metals (where s–o effect and crystal field effects were considered as equally important perturbations) shows the opposite sign of the calculated anisotropy of iron than the experimental result unless crystal field effects are included (*36*). The importance of the crystal field contribution indicates that to obtain the correct value of the anisotropy, very accurate, fully relativistic, self-consistent calculations ought to be performed, where the crystal field effect is automatically included. Some progress has been made in this direction recently, but unfortunately limited by computer resources (*37, 38*).

Thus in the present work we do not focus on self-consistent calculations of the anisotropy constants but rather on finding out what is the origin of the large magnetcrystalline anisotropy in YCo_5.

In our previous work (*39*) using a simplified single-ion crystal field model (to describe local magnetocrystalline anisotropy of cobalt) it has been shown that the large anisotropy of this compound is due to significant deviations of the c/a ratio from the ideal value $\sqrt{8/3}$.

To obtain valuable information about contributions from different sites to the anisotropy, local orbital moment calculations seem to be quite reliable even within a tight binding model (*40*). Our prediction that the Co($2c$) site has a higher orbital moment than Co($3g$) site is in concert with experimental results where a higher anisotropy contribution from Co($2c$) site has been predicted (*41*).

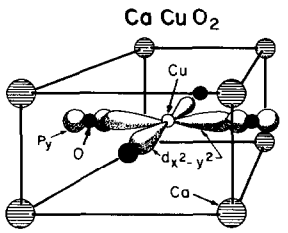

FIG. 11. The unit cell and schematic bonding for $CaCuO_2$.

Acknowledgments

This research was supported in part by the Natural Sciences and Engineering Research Council of Canada (NSERCC), NSERC, and the OCMR High T_c Consortium (Alcan, Canadian General Electric, CRAY Research and Ontario Hydro). B.S. thanks Dr. P. Strange for very close collaboration on LMTO–ASA program and its relativistic version.

References

1. C. KITTEL, "Introduction to Solid State Physics," p. 617. Wiley, New York (1963).
2. E. A. NESBITT, H. J. WILLIAMS, J. H. NERNIDE, AND R. C. SHERWOOD, *J. Appl. Phys.* **33**, 1674 (1962).

3. M. SAGAWA, S. FUJIMURA, N. TOGAWA, H. YAMAMOTO, AND Y. MATSUURA, *J. Appl. Phys.* **55,** 2083 (1984).
4. J. F. HERBST, J. J. CROAT, F. E. PINKERTON, AND W. B. YELON, *Phys. Rev. B* **29,** 4176 (1984).
5. D. GIVORD, M. S. LI, AND F. TASSET, *J. Appl. Phys.* **57,** 4100 (1985).
6. S. K. MALIK, F. J. ARLINGHAUS, AND W. E. WALLACE, *Phys. Rev. B* **16,** 1242 (1977).
7. J. C. SLATER, "Quantum Theory of Molecules and Solids; Symmetry and Energy Bands in Solids," McGraw–Hill, New York (1965).
8. J. SCHWEIZER AND F. TASSET, *J. Phys. F: Metal. Phys.* **10,** 1 (1980).
9. R. L. STREEVER, *Phys. Lett. A* **65,** 360 (1978); *Phys. Rev. B* **19,** 2704 (1979).
10. B. SZPUNAR AND W. E. WALLACE, *Lanthanide Actinide Res.* **1,** 335 (1986).
11. W. BEER AND D. G. PETTIFOR, *in* "The Electronic Structure of Complex Systems," (P. Phariseau and W. M. Temmerman, Eds.), NATO ASI Series B, Physics, p. 769. Plenum, New York (1984).
12. K. KURIHARE, S. OHTSUKA, T. UKAI, AND N. MORI, *Physica B* **130,** 317 (1985).
13. V. HEINE, D. W. BULLETT, R. HAYDOCK, AND M. J. KELLY, *Solid State Phys.* **35,** (1980).
14. B. SZPUNAR, *J. Phys. F: Metal Phys.* **12,** 759 (1982); *Physica B* **130,** 29 (1985); B. SZPUNAR AND J. SZPUNAR, *J. Appl. Phys.* **57,** 4130 (1985).
15. B. SZPUNAR, *Phys. Lett. A* **115,** 157 (1986).
16. J. CALLAWAY, "Quantum Theory of Solids," Academic Press, San Diego (1974).
17. F. HERMAN AND S. SKILLMAN, "Atomic Structure Calculations," Prentice–Hall, Englewood Cliffs, NJ (1963).
18. D. S. SAXON, "Elementary Quantum Mechanics," Holden–Day, San Francisco (1968).
19. O. K. ANDERSEN, *Phys. Rev. B* **12,** 3060 (1975).
20. H. L. SKRIVER, "The LMTO Method," Springer, Berlin (1984).
21. O. K. ANDERSEN, O. JEPSEN, AND D. GLÖTZEL, *in* "Highlights of Condensed Matter Theory," Proceedings of the International School of Physics, Enrico Fermi, Varenna, July 1983 (F. Bassani *et al.*, Eds.), Elsevier, Amsterdam (1985).
22. V. VON BARTH AND L. HEDIN, *J. Phys. C* **5,** 1629 (1972).
23. B. SZPUNAR AND P. STRANGE, *J. Phys. F: Metal Phys.* **15,** L165 (1985).
24. D. GIVORD, J. LAFOREST, R. LEMAIRE, AND Q. LU, *J. Magn. Magn. Mater.* **191,** 31 (1983).
25. M. CYROT AND M. LAVAGNA, *J. Phys.* **40,** 763 (1979).
26. T. JARLSBORG AND M. PETER, *J. Magn. Magn. Mater.* **42,** 89 (1984).
27. e.g., K. H. J. BUSCHOW, *Rep. Prog. Phys.* **40,** 1179 (1977).
28. C. KOENIG, N. E. CHRISTENSEN, AND J. KOLLAR, *Phys. Rev. B* **29,** 6481 (1984).
29. K. C. HASS, *Solid State Phys.* **42,** 213 (1989); W. E. PICKETT, *Rev. Mod. Phys.* **61,** 433 (1989); **61,** 749E (1989).
30. X. GUO, A. J. FREEMAN, AND J. YU, *Bull. Amer. Phys. Soc.* **33(M77),** 608 (1988).
31. T. SIEGRIST, S. M. ZAHURAK, D. W. MURPHY, AND R. S. ROTH, *Nature (London)* **334,** 231 (1988); D. VAKNIN, E. CAIGNOL, P. K. DAVIES, J. E. FISCHER, D. C. JOHNSTON, AND D. P. GOSHORN, "Antiferromagnetism in $(Ca_{0.85}Sr_{0.15})CuO_2$, the Parent of the Cuprate Family of Superconducting Compounds," University of Pennsylvania. [Preprint]
32. B. SZPUNAR, V. H. SMITH, JR., AND R. W. SMITH, *Physica C* **152,** 92 (1988).
33. M. R. NORMAN, *Phys. Rev. Lett.* **64,** 1162 (1990).
34. H. BROOKS, *Phys. Rev.* **58,** 909 (1940).
35. A. P. CRACKNELL, *J. Phys. C: Solid State Phys.* **2,** 1425 (1969).
36. H. J. F. JANSEN, *Phys. Rev. B* **38,** 8022 (1988); *J. Appl. Phys.* **64,** 5604 (1988).
37. H. ECKARDT, L. FRITSCHE, AND J. NOFFKE, *J. Phys. F* **17,** 943 (1987).
38. P. STRANGE, J. B. STAUNTON, M. EBERT, AND B. L. GYORFFY, [PREPRINT]; H. EBERT, P. STRANGE, AND B. L. GYORFFY, *J. Appl. Phys.* **63,** 3052 (1988).
39. B. SZPUNAR AND P. A. LINDGARD, *J. Phys. F* **9,** L55 (1979).
40. B. SZPUNAR AND W. E. WALLACE, *Phys. Rev. B* **35,** 1988 (1987); *Phys. Rev. B* **36,** 3782 (1987).
41. F. ROTHWARF, H. A. LEUPOLD, J. GREEDAN, W. E. WALLACE, AND D. K. DAS, *Int. J. Magn.* **4,** 267 (1973); J. Laforest and J. S. Shah, *IEEE Tran. Mag.* **MAG-9,** 217 (1973); K. S. V. L. NARASIMHAN, C. DO-DINH, W. E. WALLACE, AND R. D. HUTCHENS, *J. Appl. Phys.* **46,** 4961 (1975).